Comparative Study of Individual and Collective Rotational Motion in Mixtures of Liquid Crystalline Side Group Polymers and Low Molecular Weight Mesogens†

H. Seiberle, W. Stille, and G. Strobl*

Fakultät für Physik, Universität Freiburg, 7800 Freiburg, Federal Republic of Germany.
Received July 26, 1989; Revised Manuscript Received October 6, 1989

ABSTRACT: Relations between the time scales of individual and collective rotational motion of mesogenic groups were analyzed in a combined dielectric and viscosimetric study. Measurements were conducted on mixtures of liquid crystalline (LC) side group polysiloxanes and the corresponding low molecular weight compounds. The rotational diffusion constant D_r was derived from the frequency f_δ of the dielectric δ process, taking into account the retarding force of the nematic field. The time scale of collective rotation processes is set by the rotational viscosity γ_1; γ_1 was determined by a director reorientation experiment in a magnetic field. Experiments were performed under variation of the temperature and the composition of the mixture. The temperature dependencies of D_r and γ_1 are both mainly determined by that of the rotational friction coefficient $\zeta_r(T)$. $\zeta_r(T)$ is given by a Vogel–Fulcher formula. The effect of the nematic mean field on f_δ and γ_1 is correctly described by theories. In the polymer coupling of the LC groups leads to an enhanced increase of the viscosity, which is stronger than the decrease of D_r.

Introduction

Lateral attachment of mesogenic groups to a polymeric backbone chain results in a novel class of liquid crystalline materials,[1,2] the LC side group polymers. Comparison to conventional low molecular weight liquid crystals shows specific differences in structure and dynamics. They are generally due to the coupling of the mesogenic groups, which introduces positional correlations and decreases the molecular mobility. Positional correlations were first indicated by neutron scattering experiments, which showed an anisotropic conformation of the backbone chain.[3] The reduced mobility becomes apparent in the observed increase in the viscosity.

In order to analyze these polymer-specific effects in more detail we have conducted a study on the structure and rotational dynamics of a LC side group polysiloxane. In a first part of the work the molecular structures of the different phases were investigated by X-ray scattering.[4] As it turned out, layer structures are stabilized in general and become the dominating element through all mesophases and even in the isotropic melt. The structure of the nematic phase is qualitatively different from a classical nematic with random positional order. It is built up of curved layers. In the isotropic melt the short-range order remains layerlike.

The second part of the work is presented here. It deals with the kinetics of individual and collective rotational motion of the LC groups in the nematic phase. Individual rotations can be studied by dielectric relaxation. Evaluation of measurements, taking into account the retarding effect of the nematic mean field, yields the rotational diffusion constant D_r. Collective rotational motions occur in a reorientation of the nematic director. The reorientation times are controlled by the rotational viscosity γ_1.

For low molecular weight liquid crystals D_r and γ_1 are directly related by theory in a rather simple way. For polymers modifications are to be expected. This is already evident from considering the better known case of translational motions. Here the monomer mobilities, which are usually given by their reciprocals, the monomeric friction coefficients, change only slowly with the molecular weight. This is in contrast to collective properties like the viscosity, which shows a pronounced power law dependence, $\eta \sim M^\alpha$.[5] Qualitatively similar differences should be present for the rotational motions in the LC side group polymers.

The study has been performed on mixtures of a LC side group polysiloxane with the corresponding low molecular weight nematogens. Here variation of the composition enables a continuous change in viscosities over several orders of magnitude. We have compared the changes in the rotational viscosity with those of the rotational diffusion constant, which can be derived from the relaxation frequency of the dielectric δ-process, and discuss in particular the temperature dependencies of these two quantities.

Experimental Section

The polymer under investigation ("SiC_4") has the structural unit

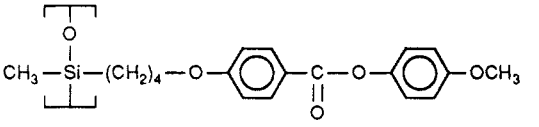

It was mixed with the low molecular weight nematogen ("C_6C_3")

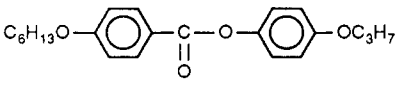

The substances were synthesized by the group of Prof. H. Finkelmann, Institut für Makromolekulare Chemie, Universität Freiburg.

The two components show complete miscibility in the isotropic and nematic phases.[6] Figure 1 gives the phase diagram derived from calorimetric measurements. The polymer has a broad molecular weight distribution with an average degree of polymerization $P_w \approx 100$.

† Dedicated to Professor E. W. Fischer on the occasion of his 60th birthday.

0024-9297/90/2223-2008$02.50/0

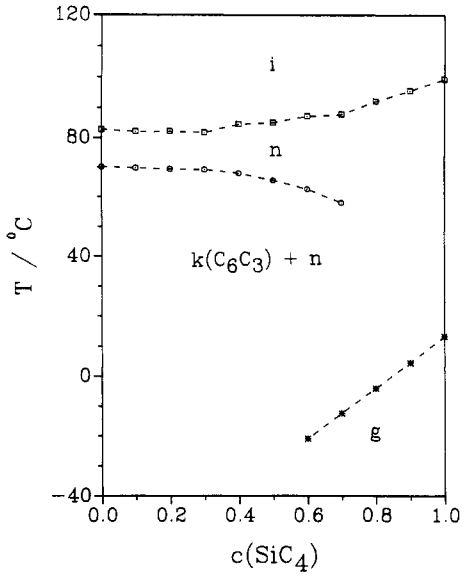

Figure 1. SiC_4/C_6C_3 mixtures. Phase diagram derived from DSC measurements.

Dielectric relaxation was studied by using the Hewlett-Packard impedance analyzer HP 4192 A. Measurements cover the frequency range f = 100 Hz–10 MHz and the temperature region T = 150–400 K. Samples had a thickness of 75 μm and were kept between gold-coated quartz plates. Cells were filled at elevated temperatures in the isotropic phase by using capillary forces. For separate measurements of $\epsilon^*_\parallel$ and $\epsilon^*_\perp$, the complex dielectric constants parallel and perpendicular to the director, samples were oriented by a magnetic field ($B \approx 1$ T). Orientation was complete, as shown by characteristic details of the relaxation behavior (absence of the δ process in $\epsilon^*_\perp$).

Rotational viscosities were determined by time-dependent dielectric measurements using a lock-in amplifier at a frequency f_0 = 50 kHz. Samples were first oriented in the magnetic field and then quickly turned by 10° into an orientation with an angle of 45° between the electric and magnetic fields. The successive reorientation of the director was followed by measuring $\epsilon'(t)$. Comparison of the torques per volume caused by the magnetic field and the rotational friction leads to the "equation of motion" for the nematic director

$$\gamma_1 \frac{d\varphi}{dt} + \frac{\Delta\chi B^2}{\mu_0} \sin\varphi \cos\varphi = 0 \tag{1}$$

where φ denotes the angle between the director and the magnetic field. γ_1 is the rotational viscosity and $\Delta\chi$ is the anisotropy $\chi_\parallel - \chi_\perp$ of the diamagnetic susceptibility. This equation is solved by[7]

$$\tan\varphi = \tan\varphi(0) \exp(-t/\tau_R) \tag{2}$$

with a reorientation time

$$\tau_R = \mu_0\gamma_1/(\Delta\chi B^2) \tag{3}$$

From the geometry described above the time dependence of ϵ' is given by

$$\epsilon'(t) - \epsilon'(\infty) = (\epsilon'_\parallel - \epsilon'_\perp)\frac{\tan\varphi(t)}{1 + \tan^2\varphi(t)} \tag{4}$$

A derivation is given in the Appendix. For sufficiently small values of φ, when $\tan^2\varphi \ll 1$, the approximation

$$\epsilon'(t) - \epsilon'(\infty) = (\epsilon'_\parallel - \epsilon'_\perp)\tan\varphi(t) = (\epsilon'_\parallel - \epsilon'_\perp)\tan\varphi(0) \times \exp(-t/\tau_R) \tag{5}$$

is valid. Measurements of τ_R yield the rotational viscosity γ_1 divided by $\Delta\chi$.

In addition, we have determined the T dependence of the order parameter S in the nematic phase of the polymer and of the low molecular weight compound. S was derived from measurements of the birefringence using an Abbé refractometer.

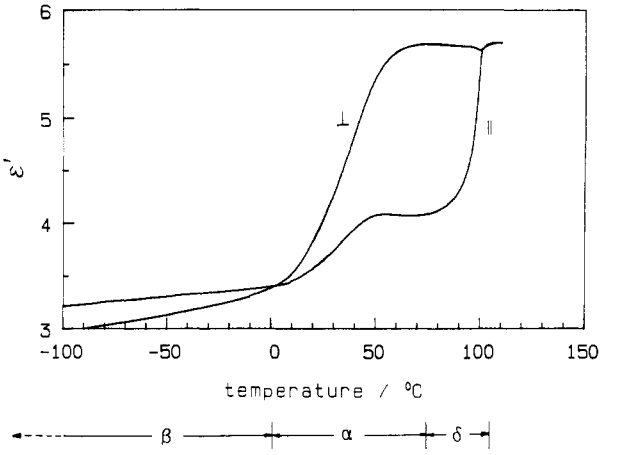

Figure 2. LC side group polymer "SiC_4". T dependence of the dielectric constants $\epsilon_\parallel$ and $\epsilon_\perp$ parallel and perpendicular to the director, measured at 10^5 Hz. Three relaxation processes, β, α, and δ, show up.

The results can be empirically described by power laws:

$$S(T) = (1 - T_r)^\nu, \quad T_r = T/T_{ni} \tag{6}$$

$$\nu(SiC_4) = 0.184, \quad \nu(C_6C_3) = 0.168$$

Transition temperatures were determined by DSC measurements. Values of T_g were obtained for all mixtures that could be quenched without a crystallization of C_6C_3. A Perkin-Elmer DSC-4 was used.

Results

Dielectric Relaxation of the LC Polymer. As is known from the literature,[8-11] LC side group polymers exhibit a complex dielectric spectrum, which is set up by different groups of relaxation processes. Figure 2 shows the real parts of the dielectric constants $\epsilon'_\parallel$ and $\epsilon'_\perp$ for the polymer under study in T-dependent runs at fixed frequency ($f = 10^5$ Hz). With increasing temperature three relaxation processes, denoted β, α, and δ, become successively activated.

The δ-process contributes exclusively to the polarization along the director. It can be associated with the longitudinal component of the dipole moment (parallel to the long axis of the mesogenic group) and the slowest mode of relaxation of its orientational distribution function. The δ-process is affected by the nematic potential. A mean-field treatment of its kinetics, which combines the Maier–Saupe theory with the Debye theory of rotational relaxation, has been given by Martin et al.[12] The α- and β-processes show up in both polarization directions, the higher relaxation strength being observed perpendicular to the director. These processes have to be mainly associated with motions of the transverse component of the dipole moment. There could also be a small contribution of the longitudinal component of the dipole moment to $\epsilon^*_\perp$, as is predicted by the theory of Martin et al.[12]

Figure 3 shows spectra $\epsilon'_\parallel(f)$ and $\epsilon''_\parallel(f)$ measured for the δ-process in frequency-dependent scans. The decrease in relaxation strength at 98 °C is due to the nematic–isotropic phase transition. The results are indicative of a simple relaxation process with a well-defined relaxation time. Figure 4 presents the Cole–Cole plot ϵ'' versus ϵ'. The center of the Cole–Cole circle shows only a small deviation from the abscissa, corresponding to a Cole–Cole function

$$\Delta\epsilon^*(\omega) = \Delta\epsilon/(1 + i\omega\tau)^{1-a} \tag{7}$$

with a = 0.08.

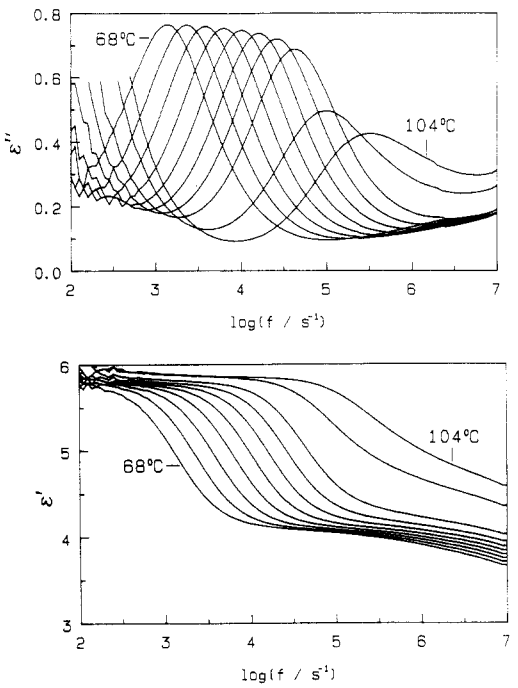

Figure 3. SiC_4. Dielectric spectra $\epsilon'_{\parallel}(f)$, $\epsilon''_{\parallel}(f)$ measured for the δ-process in the isotropic and nematic phases. Temperatures change between 68 and 104 °C in steps of 4 °C.

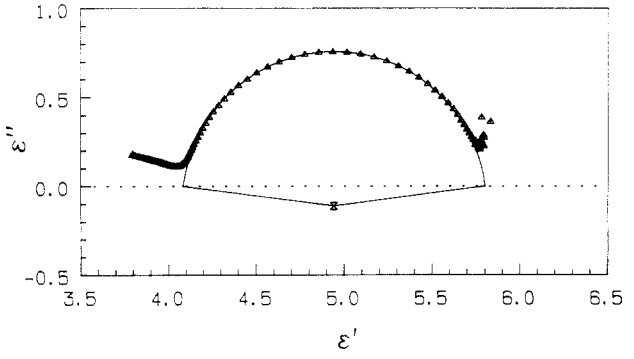

Figure 4. SiC_4. δ-Process at T = 80 °C. Cole–Cole representation of data.

The α- and β-processes (Figure 5) are more complex. There is a strong overlap and a broad distribution of relaxation times for both processes. A possible separation is indicated in Figure 6 for the spectrum obtained at T = 30 °C. The asymmetric shape of the α-process is represented here by the Havriliak–Negami function

$$\Delta\epsilon^* = \Delta\epsilon/(1 + (i\omega\tau)^{1-a})^b \qquad (8)$$

This function is a generalization of the Cole–Cole function, obtained by introducing a second parameter b. The parameter values of the fit in Figure 6 are a = 0.35 and b = 0.5.

The shape of the curves is similar to that found for the dielectric α-process in simple polymers. There it is understood as reflecting a group of cooperative processes that freeze at the glass transition. The β-process apparently changes its form with temperature. The sum of the relaxation strengths of the α- and β-processes is practically constant. So far a more detailed understanding of the microscopic nature of the α- and β-processes has not been achieved. This is directly related to the lack of basic understanding of the glass transition.

Figure 7 presents the temperature dependence of the δ- and α-processes by using an Arrhenius plot. Coupling of the α-process to the glass transition is evident from

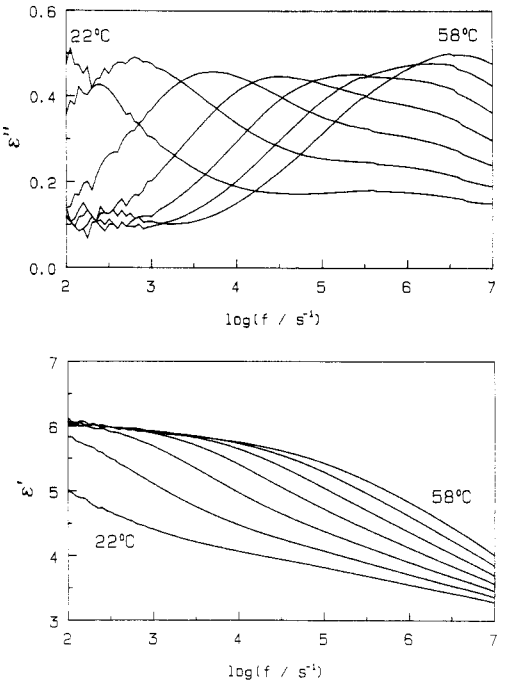

Figure 5. SiC_4. Dielectric spectra $\epsilon'_{\perp}(f)$ and $\epsilon''_{\perp}(f)$ measured for the α- and β-processes in the nematic phase (T = 22–58 °C in steps of 6 °C).

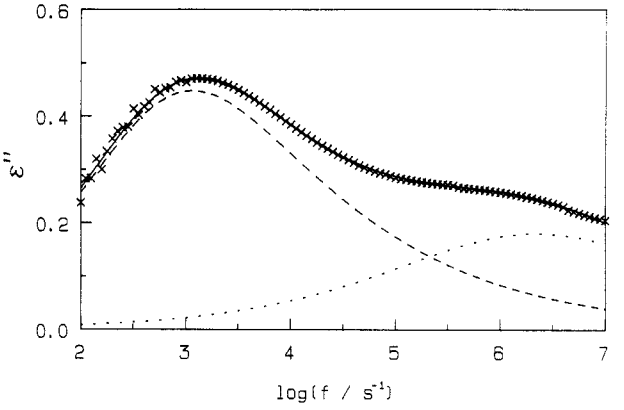

Figure 6. SiC_4. Separation of a spectrum (T = 30 °C) into a α- and β-contributions.

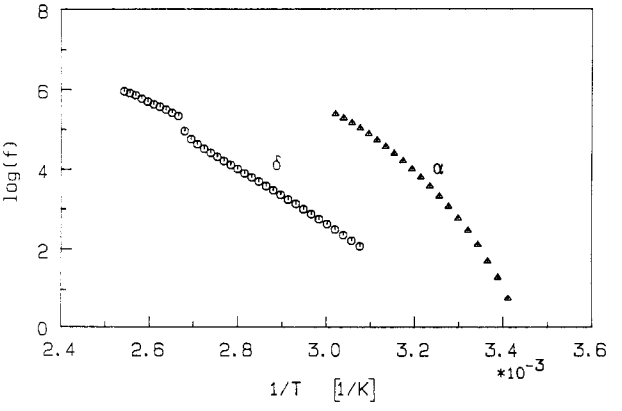

Figure 7. SiC_4. Arrhenius plot showing the T dependence of the relaxation frequencies of the α- and δ-processes.

the characteristic curvature. At a first glance the behavior of the δ-process appears different. This, however, is an incorrect impression. The frequencies of the δ-process are affected by the nematic potential as described by the Martin–Meier–Saupe theory.[12] This effect has to be accounted for; we shall come back to this point later

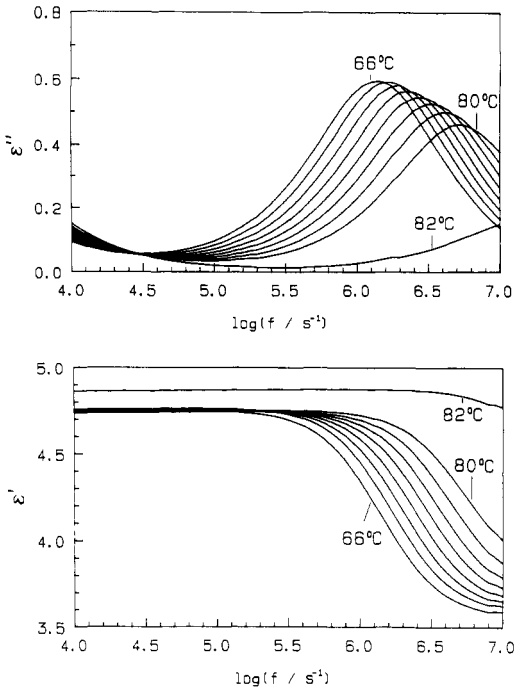

Figure 8. Low molecular weight mesogen "C_6C_3". Dielectric spectra $\epsilon'_{\parallel}(f)$ and $\epsilon''_{\parallel}(f)$ of the δ-process, measured in the nematic phase (T = 66–80 °C in steps of 2 °C).

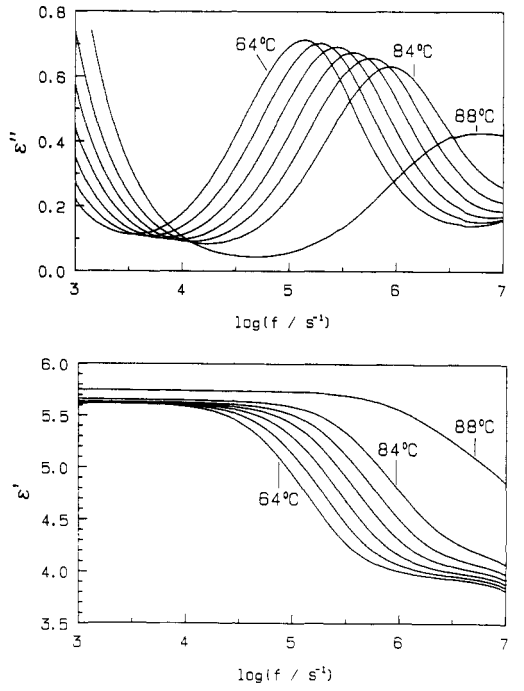

Figure 9. SiC_4/C_6C_3 (1:1) mixture. Dielectric spectra $\epsilon'_{\parallel}(f)$ and $\epsilon''_{\parallel}(f)$ of the δ-process, measured in the nematic phase (T = 64–84 °C in steps of 4 °C).

on. There are also two studies, one performed on a low molecular weight compound[13] the other on a polymer sample,[14] that follow the δ-process to lower frequencies. Both show curved Arrhenius plots, thus providing evidence that not only the α-process but also the δ-process is coupled to the glass transition.

Dielectric Relaxation of LC Polymer/Low Molecular Weight Mesogen Mixtures

Figure 8 shows dielectric spectra of the δ-process of the low molecular weight compound C_6C_3 in the nematic phase. The relaxation frequencies are about three decades higher than those of the corresponding LC polymer SiC_4. Line shapes correspond to a simple relaxation process with a unique relaxation time.

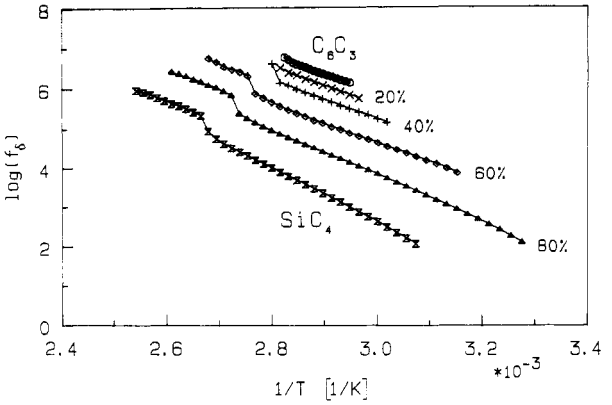

Figure 10. Series of SiC_4/C_6C_3 mixtures. T dependence of the δ-relaxation frequency.

Figure 9 presents the δ-spectra of a SiC_4/C_6C_3 (1:1) mixture. Only one process is observed, with a relaxation frequency located between those of SiC_4 and C_6C_3. The line width, and also the relaxation strength, are similar to those of pure SiC_4 (Cole–Cole parameter $a \approx 0.10$). Equivalent spectra were observed for the other samples in the series of mixtures. With increasing polymer fraction $c(SiC_4)$ frequencies f_δ decrease continuously. Results are collected in the Arrhenius plots in Figure 10. The apparent activation energy $d \ln f_\delta/d(1/T)$ increases with $c(SiC_4)$.

For the majority of the blends a measurement of the frequencies of the α- and β-processes over an extended temperature range in the nematic phase was not possible. The low molecular weight component crystallized at lower temperatures.

Rotational Viscosities of LC Polymer/Low Molecular Weight Mesogen Mixtures

Figure 11 shows the time dependence of the dielectric constant $\epsilon'(t)$ after an angular displacement, keeping the sample in the magnetic field. One observes an exponential transition into the new equilibrium state, as described by eq 5

$$[\epsilon'(t) - \epsilon'(\infty)]/[\epsilon'(0) - \epsilon'(\infty)] = \exp(-t/\tau_R)$$

The values of $\gamma_1/\Delta\chi$ obtained for the whole series of SiC_4/C_6C_3 mixtures in the nematic phase are presented in Figure 12. Viscosities increase with the polymer fraction and with decreasing temperature.

Temperature and Order Parameter Dependence of Rotational Motion

First we give a summary of some relevant theoretical results.

The basic time scale for rotational motions is set by the rotational diffusion constant D_r. It describes for this discussion of single mesogenic molecules and LC side groups, the orientational motion of the long axis. D_r is usually introduced as the leading factor in the Smoluchowski equation of Brownian rotational motion (compare, e.g., ref 15)

$$\frac{\partial\psi(\vec{u},t)}{\partial t} = D_r K\psi \qquad (9)$$

with $\psi(\vec{u},t)$ the orientational distribution function ($\vec{u}$ is

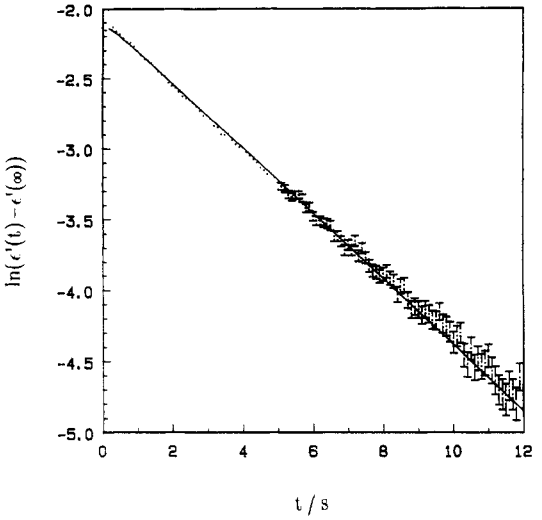

Figure 11. SiC_4/C_6C_3 (1:1) mixture in the nematic phase (T = 60 °C). Time dependence of dielectric constant $\epsilon'(t)$ after an angular displacement in a magnetic field.

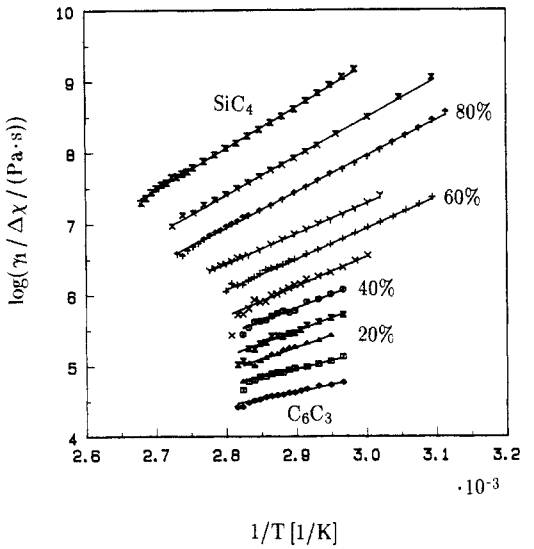

Figure 12. Series of SiC_4/C_6C_3 mixtures in the nematic phase. T dependence of $\gamma_1/\Delta\chi$ (γ_1, rotational viscosity; $\Delta\chi$, anisotropy of diamagnetic susceptibility).

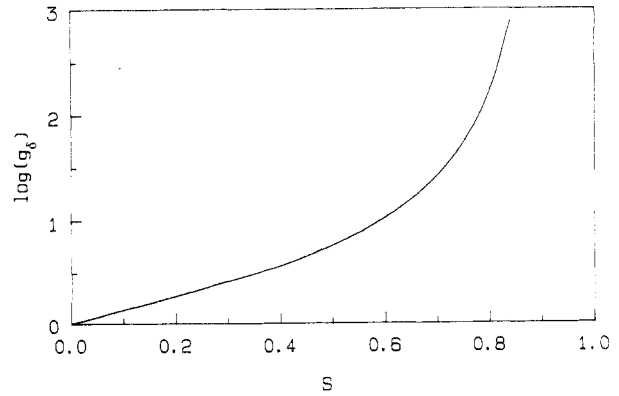

Figure 13. Retardation factor $g_\delta(S)$, as given by the Martin–Meier–Saupe theory.[12]

a unit vector giving the direction of the long axis) and K the dynamical operator effective for the system. In the isotropic phase D_r determines the correlation function of the orientational motion

$$\langle \tilde{u}(0)\, \tilde{u}(t) \rangle = \exp(-2D_r t) \tag{10}$$

and specifies the mean-squared displacement of the orientation vector, which for short times is given by

$$\langle (\tilde{u}(t) - \tilde{u}(0))^2 \rangle = 4D_r t \tag{11}$$

D_r can be associated with the rotational mobility ν_r, which is defined as

$$\vec{\omega} = \nu_r \vec{N} \tag{12}$$

with $\vec{\omega}$ the angular velocity of $\tilde{u}$ and $\vec{N}$ the torque exerted by an external field. The relation is given by Einstein's law

$$D_r = kT\nu_r \tag{13}$$

If rodlike particles are rotated in a viscous solvent, ν_r depends on the rod length L and the viscosity η_s of the solvent essentially as

$$\nu_r \cong 1/(\eta_s L^3) \tag{14}$$

Equation 14 provides a good description for rodlike colloids with high aspect ratio in dilute solution.[15] For this discussion of the rotational motion of mesogenic molecules and polymer side groups in the bulk, η_s has to be replaced by the microscopic local viscosity effective in the bulk. The dependence on the rod length is different from that in dilute solutions and not known from theory. Therefore the dependencies on the viscosity and L are no longer treated separately. Usually a rotational friction coefficient ζ_r is introduced, which is defined as the reciprocal value of ν_r[15]

$$\nu_r = 1/\zeta_r \tag{15}$$

The definition is analogous to that of the monomeric friction coefficient used in treatments of translational segmental motion.[5,15] Replacement of ν_r by ζ_r in eq 13 gives

$$D_r = kT/\zeta_r \tag{16}$$

Both, the δ-relaxation frequency f_δ and the rotational viscosity γ_1 are related to D_r. The Martin–Meier–Saupe treatment[12] yields for f_δ

$$2\pi f_\delta = 2D_r/g_\delta(S) \tag{17}$$

The "retardation factor" $g_\delta(S)$ describes the effect of the nematic potential, which leads to a decrease of f_δ. $g_\delta(S)$ depends only on the order parameter and has the limiting values $g_\delta(S{=}0) = 1$ and $g_\delta(S{\to}1) \to \infty$. Although there is no analytic equation we found that for $S < 0.8$ the expression

$$\log g_\delta(S) = 1.069S + 0.113/(1 - S)^{1.609} - 0.106 \tag{18}$$

provides a good representation of the numeric values. Figure 13 shows this dependence.

Hess[16] has derived the following equation for the rotational viscosity γ_1 of low molecular weight nematogens:

$$\gamma_1 = 5\rho kT/(g_\gamma(S)2D_r) \tag{19}$$

with

$$g_\gamma(S) = S^{-2} \tag{20}$$

ρ denotes the particle density. Equations 19 and 20 find support in experiments by Kneppe et al.[17]

For polymers, coupling of the LC groups by the backbone chain will result in an increase of the rotational viscosity γ_1. This is due to two different factors: (i) The local microscopic viscosity will increase, leading to a lower value of the rotational diffusion constant D_r. (ii) There

is a second factor, which is not included in eq 19. For polymers reorientation of the director field cannot be accomplished just by a superposition of individual rotational motions of the LC side groups. It necessarily includes a rearrangement of the backbone chain together with additional translational motions of the mesogens. We therefore assume for the polymer case and the mixtures a modified equation for γ_1:

$$\gamma_1 = C5\rho kT/(g_\gamma(S)2D_r) \tag{21}$$

were C denotes an empirical "connectivity factor", which accounts for the effect of the backbone chain.

Equations 17 and 21 show that the temperature dependence of f_δ and γ_1 is mainly determined by the T dependence of D_r. The rotational friction coefficient ζ_r and therefore ν_r are coupled to the glass transition and follow a Vogel–Fulcher law

$$\zeta_r = \zeta_r^0 \exp\left(\frac{A}{T - T_0}\right) \tag{22}$$

$$\nu_r = \nu_r^0 \exp\left(-\frac{A}{T - T_0}\right) \tag{23}$$

The limiting temperature T_0 is usually located 30–70 K below the dilatometric glass transition temperature T_g. D_r follows from eq 13:

$$D_r = kT\nu_r^0 \exp\left(-\frac{A}{T - T_0}\right) = D_r^0 \exp\left(-\frac{A}{T - T_0}\right) \tag{24}$$

The prefactors ζ_r^0, ν_r^0, and D_r^0 change slowly with temperature. Different expressions have been proposed in the literature. The changes following from the different formulas are always small in comparison to those associated with the dominating exponential term. Therefore, in evaluations of data obtained in a restricted temperature range, the prefactors are usually treated as constants.

An additional T dependence is contributed by $g_\delta(S(T))$ and $g_\gamma(S(T))$. It is weak compared to that given by $D_r(T)$ but cannot be neglected. In particular, $g_\delta(S(T))$ becomes increasingly important with higher values of S, i.e., decreasing T, as is indicated by eq 18.

Discussion

First we have to address a principal point. The question is whether the reorientational motion of individual LC groups can really be considered as a single particle property, as is assumed by using the single particle rotational diffusion constant D_r as the basic quantity, or has to be treated as a result of a collective process. In fact, the observation of only one observed process in the dielectric δ-spectrum of the mixtures (Figure 9), rather than two separated ones, at first glance indicates collectivity. However, this is a wrong impression. Experiments on other mixtures, a low molecular weight mixture[18] and also a LC polyacrylate/low molecular weight mesogen mixture,[19] did show a clear splitting of the δ-process. In addition, a collective relaxation, like the α-process, always exhibits marked deviations from a single relaxation time behavior, showing usually a clear asymmetric broadening. This is not observed here. Hence, we believe that in our case the δ-relaxation rates of the polymer and monomer in the mixture are too similar to be resolved by the measurement. Basically we can deal with single-particle rotations as the elementary process.

The similarity of the relaxation frequencies, and therefore of the rotational mobilities, of the polymeric and low molecular weight LC groups is an interesting observation. Generally, mobilities are determined by the microscopic local viscosity, which is common for both components, and the size of the mobile unit. A strong coupling of the LC side groups to the polymer backbone would increase their effective size over that of the monomer component. We therefore have to conclude that for the polysiloxanes under study the coupling is weak and the decoupling of rotational motion by the spacer sequence and the highly mobile backbone chain quite efficient. This is not generally the case. As shown by the work on a LC side group polyacrylate,[19] coupling can be much stronger.

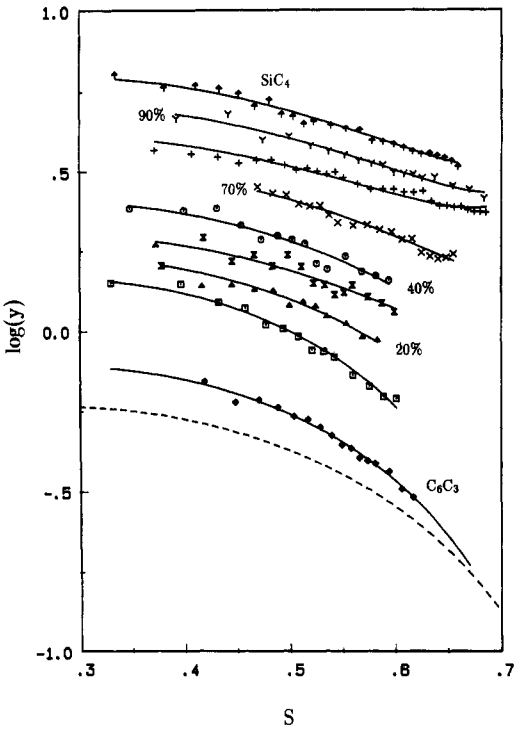

Figure 14. Series of SiC_4/C_6C_3 mixtures in the nematic phase. Plot of $y = 2\pi f_\delta \gamma_1 \Delta\chi_0/(\rho kT\Delta\chi)$ against the order parameter S. Comparison with theoretical curve valid for low molecular weight mesogens (broken line).

Principally, the decrease of f_δ with increasing polymer content could be due to either an increase of the effective size of the rotating unit or an increase in the microscopic local viscosity of the bulk medium. The observations show clearly that the latter factor is by far the dominant one. The decrease of f_δ is primarily a consequence of an increase in T_g.

In an analysis of the T dependence of γ_1 and f_δ, the different factors $D_r(T)$, g_γ or g_δ, and C have to be separated. This can be achieved by considering first the product quantity

$$y = 2\pi f_\delta \gamma_1 \Delta\chi_0/(\Delta\chi\rho kT) \tag{25}$$

y is independent of $D_r(T)$ and depends on the temperature only through the slowly changing order parameter S. Using

$$\Delta\chi = \Delta\chi_0 S \tag{26}$$

together with eqs 17 and 21 gives

$$y(S) = 5C/(g_\delta g_\gamma S) \tag{27}$$

According to eq 27 the product function $y(S)$ is determined by the retardation factors $g_\delta(S)$ and $g_\gamma(S)$, which are given by the eqs 18 and 20, and by the empirical connectivity factor C.

The experimental results are shown in Figure 14. The

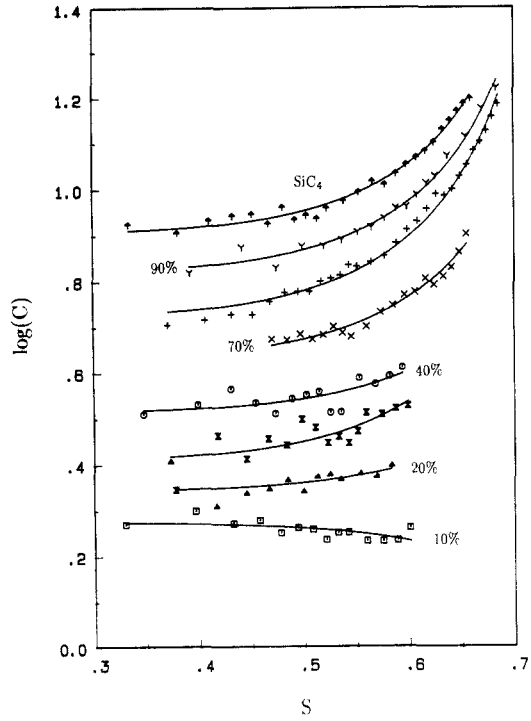

Figure 15. SiC_4/C_6C_3 mixtures in the nematic phase. Factor C describing the enhanced increase of the rotational viscosity γ_1 due to the chain connectivity.

plot includes also the theoretical function valid for pure low molecular weight mesogens ($C = 1$).

One notes for pure C_6C_3 a satisfactory agreement between theory and experiment. The shape $y(S)$ is well described by the theory; the small difference in absolute values corresponds to the uncertainty in $\Delta\chi_0$.

With increasing polymer fraction $y(S)$ shifts to higher values. The shift indicates that the increase of the rotational viscosity is larger than that of the dielectric relaxation time $(2\pi f_\delta)^{-1}$. The behavior can be formally described by use of the connectivity factor C. Values of C for the different mixtures are presented in Figure 15. They were obtained for a given mixture by dividing $y(S)$ through the values measured for pure C_6C_3 (as represented by the continuous curve shown in Figure 14). C increases with the polymer fraction.

According to Figure 15 the parameter C is a function of the order parameter S, showing larger values for higher degrees of orientational order. An explanation can be given by considering the conformation of the backbone chain. Usually the backbone chain is preferentially oriented perpendicular to the director. The anisotropy is larger for higher values of S. The extent of conformational rearrangement of the backbone chain induced by a change of the director orientation will depend on the anisotropy: for only weakly anisotropic conformations small changes are sufficient; for planar conformations the whole plane has to be rotated, which requires rather large changes. From this the observed increase in the connectivity factor can be understood.

The rotational diffusion constant D_r can be derived from the measured δ-relaxation frequency by application of eq 17. The temperature dependence $D_r(T)$ is directly related to that of the rotational friction coefficient. One expects a T dependence as described by eq 24.

Figure 16 presents the frequencies f_δ and the derived rotational diffusion constants D_r, obtained in the isotropic and nematic phase of the polymer SiC_4. The step-

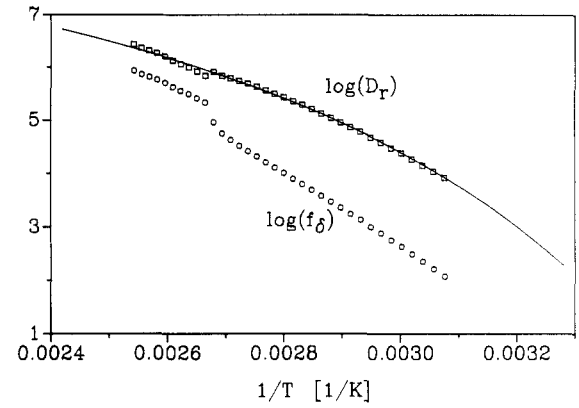

Figure 16. SiC_4. T dependencies of the δ-relaxation frequency f_δ (○) and rotational diffusion constant D_r (□).

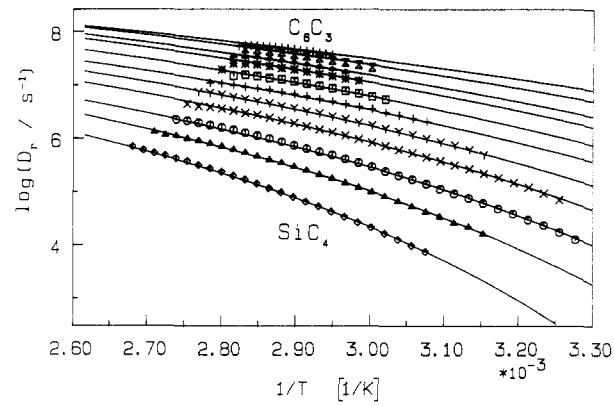

Figure 17. SiC_4/C_6C_3 mixtures. T dependence of rotational diffusion constants. Representation by the Vogel–Fulcher law (continuous lines).

like change of f_δ at the phase transition is greatly reduced for D_r. Obviously the step is largely due to the change in the order parameter from zero to a finite value. The Arrhenius plot for the temperature dependence of the rotational diffusion constant is no longer linear. It shows the curvature characteristic for processes that are coupled to the glass transition. The continuous line gives a fit on the basis of

$$D_r(T) = D_r^0 \exp\left(-\frac{A}{T - T_0}\right) \tag{24}$$

with the parameters $A = 1170$ K, $T_0 = 236$ K, and $D_r^0 = 3.86 \times 10^9$ s^{-1}. The limiting temperature T_0 is located 50 K below T_g (=286 K).

In Figure 17 the diffusion constants obtained for the whole set of mixtures are shown. Curvature of the Arrhenius plots is obvious. The continuous lines that fit the data were calculated using a common parameter $A = 1170$ K under variation of the limiting temperatures T_0 and prefactors D_r^0.

The values obtained for T_0 are shown in Figure 18. A continuous increase with growing polymer fraction is observed. Figure 18 also includes values $T_g - 50$ K for all those samples for which the glass transition temperatures could be measured by DSC (this was possible for polymer fractions larger than 60%). The results are indicative of a constant difference of 50 K between T_g and the limiting temperature T_0. Figure 19 shows all data in a common plot based on the Vogel–Fulcher expression, $\log (D_r/D_r^0)$ versus $1/(T - T_0)$. All data fall on one line.

Figure 20 gives the dependence of the prefactors D_r^0 on the polymer fraction. D_r^0 changes by 1 order of magnitude. The large difference between the diffusion con-

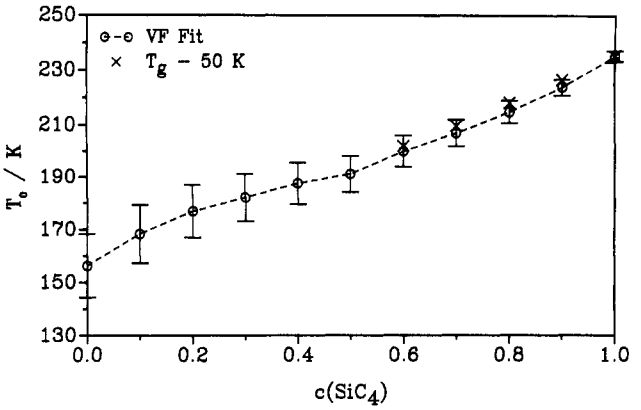

Figure 18. SiC_4/C_6C_3 mixtures. Dependence of the limiting temperature T_0 on the polymer fraction. Values of T_g - 50 K are shown, indicating a constant difference between T_0 and T_g.

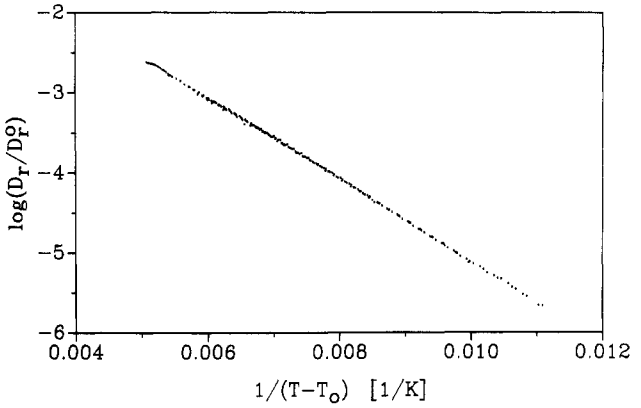

Figure 19. SiC_4/C_6C_3 mixtures. Plot of log D_r/D_r^0 versus $1/(T - T_0)$, demonstrating the validity of the Vogel–Fulcher law.

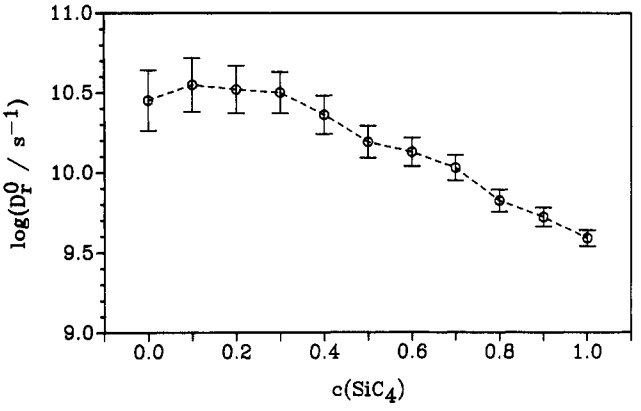

Figure 20. SiC_4/C_6C_3 mixtures. Dependence of the prefactor D_r^0 on the polymer fraction.

stants of the low molecular weight and the polymeric compound therefore originates from two sources, a shift of the glass transition temperature and a change of the prefactor D_r^0.

Conclusion

Analysis of the temperature-dependent measurements of the relaxation frequency f_δ and the rotational viscosity γ_1 for mixtures of different composition leads to the following results:

(i) The temperature dependencies of f_δ and γ_1 are mainly determined by that of the rotational diffusion constant $D_r(T) = kT/\zeta_r(T)$. $D_r(T)$ is described by the Vogel–Fulcher formula. There is a strong decrease of D_r with increasing polymer fraction. The change is due to the shift of the glass transition temperature and also a decrease of the prefactor D_r^0.

(ii) The effects of the nematic potential on f_δ and γ_1 appear to be properly described by the δ-dependent factors $g_\delta(S)$ and $g_{\gamma_1}(S)$ introduced in the theories of Martin–Meier–Saupe and Hess.

(iii) The coupling of the LC groups in the polymer leads to an enhanced increase of the rotational viscosity, which is larger than that of the dielectric relaxation time $(2\pi f_\delta)^{-1}$. In order to account for this effect an additional factor has to be introduced into the relation between γ_1 and D_r.

Acknowledgment. Support of this work by the Deutsche Forschungsgemeinschaft is gratefully acknowledged (Sonderforschungsbereich 60, Freiburg). Special thanks are due to Professor Finkelmann for providing us with samples.

Appendix

In an oriented nematic layer placed between two parallel electrodes with an angle α between the director and the layer normal the effective dielectric constant is given by

$$\epsilon' = \epsilon'_\parallel \cos^2\alpha + \epsilon'_\perp \sin^2\alpha = \epsilon'_\parallel - \Delta\epsilon' \sin^2\alpha \quad \text{(A1)}$$

with

$$\Delta\epsilon' = \epsilon'_\parallel - \epsilon'_\perp \quad \text{(A2)}$$

The reorientation measurements were performed with samples oriented parallel to a magnetic field $\vec{B}$, which then was quickly turned by 10° to the direction with an angle of 45° between electric and magnetic field. Therefore the time-dependent angle $\alpha(t)$ is then given by the angle $\varphi(t)$ between $\vec{B}$ and director $\hat{n}$:

$$\alpha(t) = \pi/4 - \varphi(t) \quad \text{(A3)}$$

Using the trigonometric formulas, we obtain for the time-dependent effective dielectric constant $\epsilon'(t)$

$$\begin{aligned}\epsilon'(t) &= \epsilon'_\parallel - \Delta\epsilon' \sin^2[\pi/4 - \varphi(t)] \\ &= \epsilon'_\parallel - (1/2)\Delta\epsilon'[\cos\varphi(t) - \sin\varphi(t)]^2 \\ &= \epsilon'_\parallel - (1/2)\Delta\epsilon' + \Delta\epsilon' \cos\varphi(t) \sin\varphi(t) \\ &= \frac{\epsilon'_\parallel - \epsilon_\perp}{2} + \Delta\epsilon' \frac{\tan\varphi(t)}{1 + \tan^2\varphi(t)} \quad \text{(A4)}\end{aligned}$$

This quantity is determined by time-dependent measurement of the imaginary part of the current through the capacitor by using a lock-in technique. A nematic liquid crystal with positive anisotropy of the diamagnetic susceptibility is oriented parallel to the magnetic field:

$$\varphi(t\to\infty) = 0 \quad \text{(A5)}$$

$$\epsilon'(\infty) = \epsilon'(t\to\infty) = \frac{\epsilon'_\parallel - \epsilon'_\perp}{2} \quad \text{(A6)}$$

Finally we obtain for the difference between $\epsilon'(t)$ and the limit $\epsilon'(\infty)$

$$\epsilon'(t) - \epsilon'(\infty) = \Delta\epsilon' \frac{\tan\varphi(t)}{1 + \tan^2\varphi(t)}$$

References and Notes

(1) Finkelmann, H.; Ringsdorf, H.; Wendorff, H. *Makromol. Chem.* **1978**, *179*, 273.
(2) Shibaev, V. P.; Plate, N. A. *Polym. Sci. USSR* **1978**, *19*, 1065.
(3) Kirste, R.; Ohm, H. *Makromol. Chem., Rapid Commun.* **1985**, *6*, 179.

(4) Hotz, W.; Strobl, G. *Colloid Polym. Sci.*, in press.
(5) Ferry, J. D. *Viscoelastic Properties of Polymers*; Wiley: New York, 1980.
(6) Benthack-Thoms, H. Dissertation; Clausthal-Zellerfeld, 1985.
(7) Heppke, G.; Schneider, F. *Z. Naturforsch.* **1972**, *27a*, 976.
(8) Kresse, H.; Talrose, R. *Makromol. Chem.*, Rapid. *Commun.* **1981**, *2*, 369.
(9) Zentel, R.; Strobl, G.; Ringsdorf, H. *Macromolecules* **1985**, *18*, 960.
(10) Haase, W.; Pranoto, H.; Bormuth, F. *Ber. Bunsenges. Phys. Chem.* **1985**, *89*, 1229.
(11) Attard, G. S. *Mol. Phys.* **1986**, *58*, 1087.
(12) Martin, A. J.; Meier, G.; Saupe, A. *Symp. Faraday Soc.* **1971**, *5*, 119.
(13) Zeller, H. *Phys. Rev. Lett.* **1982**, *48*, 334.
(14) Attard, G.; Moura-Romas, J.; Williams, G. *J. Polym. Sci., Polym. Phys. Ed.* **1987**, *25*, 1099.
(15) Doi, M.; Edwards, S. F. *The Theory of Polymer Dynamics*; Clarendon: Oxford, 1986.
(16) Hess, S. *Z. Naturforsch. A* **1975**, *30*, 1224.
(17) Kneppe, H.; Schneider, F.; Sharma, N. K. *J. Chem. Phys.* **1982**, *77*, 3203.
(18) Zeller, H. R. *Phys. Rev. A* **1981**, *23*, 1434.
(19) Kresse, H.; Stettin, H.; Kostromin, S.; Shibaev, V. *Mol. Cryst. Liq. Cryst.*, submitted for publication.

Registry No. $C_6H_{13}OC_6H_4$-*p*-$CO_2C_6H_4$-*p*-OC_3H_7, 50649-51-9.

Density Profile of Terminally Anchored Polymer Chains: A Monte Carlo Study

Amitabha Chakrabarti* **and Raul Toral†**

Department of Physics and Center for Polymer Science and Engineering, Lehigh University, Bethlehem, Pennsylvania 18015. *Received July 13, 1989; Revised Manuscript Received September 29, 1989*

ABSTRACT: We present results of a detailed Monte Carlo simulation study of a system of a large number of polymer chains terminally anchored or end-grafted on a flat surface. We study this system on a three-dimensional lattice for several different values of the surface coverage and the chain length. We also consider several different distributions for the chain lengths. For monodisperse chains, we find that the monomer density profile shows a depletion layer near the grafting plane in agreement with phenomenological theories. Beyond this depletion layer, the density profile can be represented by a parabolic form. This result is in agreement with recent self-consistent-field (SCF) calculations rather than with the scaling arguments that predict a plateau region for the density profile. The chain-end density is also found to be consistent with the SCF calculations; i.e., we find that the free ends of the chains are not excluded from regions near the grafting surface. We also study the effect of polydispersity in the chain lengths. In the case of a system consisting of two species of polymers of length N and $2N$, we find that there is a region in which the density profile matches that of the monodisperse case with chain length N, in agreement with another recent self-consistent-field calculation. The width of this region, however, is narrower than that predicted by the theory. We have also considered a uniform distribution of chain lengths and compared the density profile with the functional form obtained by intergrating the equations derived in the SCF formalism. The agreement between the Monte Carlo data and the theory is remarkable except, again, for the presence of a depletion layer near the grafting plane.

I. Introduction

The configurations of polymer chains adsorbed at a solid–liquid or liquid–liquid interface have attracted considerable interest in recent years, mainly because of their important applications in various different problems of colloidal stability, adhesion, lubrication, and biophysics. Colloidal particles are kept in suspension and often protected against flocculation by terminally anchoring (also called grafting) polymers onto their surfaces.[1-5] Since the adsorbed polymer layers repel each other, they can provide a long-range repulsion between the colloidal particles. A quantitative prediction about the interactions between the stabilized particles for different solvent qualities and polymer–surface interactions is an extremely difficult task, since this will involve a detailed knowledge of the chain conformations near the surface and a quantitative theory of polymer solution dynamics, none of which is presently attainable. As a result, previous theoretical treatments of surfaces bearing terminally attached polymer chains have employed various approximate schemes, such as Flory-type mean-field arguments,[6] phenomenological scaling arguments,[7] and self-consistent-field (SCF) methods.[8-10] Among these various approaches, the SCF methods seem to be in better agreement with the experimental observations.[11]

Both Flory-type arguments of Alexander[6] and scaling arguments of de Gennes[7] note that, under good solvent conditions and high enough surface coverage σ, allowing overlap between individual chains, the chains will be stretched, for the case of nonadsorbing grafting surfaces. These theories do not provide an explicit form for the equilibrium monomer density profile as a function of distance z from the grafting plane (measured in units of monomer size a). The qualitative features are

* Present address: Department of Physics, Kansas State University, Manhattan, KS 66506.
† Permanent address: Departament de Fisica, Universitat de les Illes Balears, Palma de Mallorca, E-07071 Spain.

0024-9297/90/2223-2016$02.50/0